Structure and thermodynamic properties of liquid transition metals: An embedded-atom-method approach

G. M. Bhuiyan
Department of Physics, Dhaka University, Dhaka 1000, Bangladesh

M. Silbert*
School of Physics, University of East Anglia, Norwich NR4 7TJ, United Kingdom

M. J. Stott
Department of Physics, Queen's University, Kingston, Canada K7L 3N6
(Received 3 April 1995; revised manuscript received 1 August 1995)

We have obtained the volume term and effective pair potentials for liquid transition metals using the embedded-atom method (EAM). The EAM embedding functions are fitted to bulk solid-state properties: the experimental Voigt average bulk and shear moduli and sublimation energies. The same fitting procedure is used for all the transition metals. This potential is used in conjunction with the variational modified hypernetted chain (VMHNC) theory of liquids to compute the static structure factors, Helmholtz free energies, internal energies, and entropies of the $3d$, $4d$, and $5d$ liquid transition metals. There is overall good qualitative agreement with experiment. The computed thermodynamic properties exhibit trends in accordance with experiment. They also exhibit the correct behavior as a function of temperature. But the calculations also reveal shortcomings in the interatomic potential.

I. INTRODUCTION

This paper presents a detailed study of the structure and thermodynamic properties of liquid transition metals. We show below that a volume term in the energy plus effective pair potentials obtained from the embedded atom method[1,2] (EAM) combined with an accurate theory of liquids, the variational modified hypernetted chain theory[3,4] (VMHNC) provide a sound basis for the prediction of both liquid structure and thermodynamic properties.

Recent theoretical work on liquid transition metals used the effective pair potentials of Wills and Harrison[5] (WH), which are based on a separate treatment of the s-p and d states and, in addition, take account of the effect of s-d hybridization. The use of the WH potential, in conjunction with thermodynamic perturbation theories to describe liquid structure, led to promising results.[6,7] However, when the full WH potential is used together with accurate liquid-state theories,[8,9] it fails to produce results for the structure factor $S(q)$ of the $3d$ transition metals with half- and less-than-half-filled d bands. Moreover, molecular dynamics (MD) simulations[9] using the WH potentials fail to produce reasonable results for the structure of liquids Ti and V.

It has been suggested[9] that the difficulties encountered with the use of the WH potential are because of the position and very deep first minimum of its potential well (which is larger than the thermal energy). These deficiencies have been attributed to the crudeness of the WH treatment of s-d hybridization as well as the neglect of multiple-ion potentials. Yet, potentials recently developed, using the generalized pseudopotential theory[10] (GPT), which include multiple-ion contributions, encounter similar difficulties in liquid-state calculations.[11] A thorough MD study of molybdenum[12] shows that, using Moriarty's potential, the system melts at $T_m=3528$ K, whereas the experimental melting temperature is $T_m=2883$ K. Actually these multiple-ion interatomic potentials obtained from first-principles GPT have potential wells that are even deeper and placed at smaller values of r than the WH potentials.

Progress along the lines pioneered by Wills and Harrison was made by developing a new simple effective pair interaction for the liquid transition metals, which, following WH, used a local form constructed by the superposition of the s-p and d states, but with the latter deduced from an inverse scattering approach.[13] The results for the liquid structure factors, obtained using this potential, in conjunction with the VMHNC theory of liquids,[14] agree reasonably well with the experimental x-ray diffraction for the $3d$ series.[15] However, when the same approach was used to calculate the thermodynamic properties of the $3d$ liquid transition metals, the results did not show the experimental trends.[16] This result is not unexpected, as it has long been suggested that potentials derived from local pseudopotentials are not capable of predicting the energetics of liquid transition metals.[17]

A recent study of the structure of the $3d$ liquid transition metals[18] in which the effective pair potential has been obtained by using the tight-binding cluster Bethe lattice method where the role of the s-p electrons, including hybridization, is treated self-consistently. The results of using this approach for the liquid structure and electronic density of states are promising. However, it remains to be seen whether it can also account for the experimental trends of thermodynamic properties and also give a satisfactory account of the properties of the $4d$ and $5d$ rows of the liquid transition metals.

A combined study of both the structure and thermodynamic properties of the liquid transition metals has to overcome the difficulties indicated above, and we use interatomic

potentials derived from the EAM for these purposes. This model stems from the density-functional-based quasiatom model,[19] in which the band structure and, in particular, the d bands do not appear explicitly, and which also includes multiple-ion interactions. Its possible use for the study of liquid transition metals was suggested in the conclusion of the first, albeit crude, detailed study of their thermodynamic properties.[20] Foiles[21] was the first to have done so in a paper where he presented MD results for the liquid structure of the late transition and noble metals, which are in good agreement with the experimental data.

There are a number of other papers that have also used EAM potentials in MD simulations of, mainly, the liquid structure of a number of transition metals,[22–25] except for one, which studies the thermodynamic properties of the late $3d$ series.[26] However, to the best of our knowledge, the work presented below is the first systematic study that encompasses both the structure and thermodynamics of *all* the transition metals in their liquid state near melting.

Our approach is based on the premise that, given the isotropy and homogeneity of the liquid state, we can use the same parametrization for all the transition metals, irrespective of the series they are in or their parent crystallographic solid-state structure. A systematic prescription is then used for the determination of approximate pair potentials from the EAM. It is these pair potentials that are used in conjunction with the VMHNC liquid-state theory to predict both the liquid structure and thermodynamic properties. We note that once the EAM parameters have been determined from solid-state properties, the ensuing theory is free from adjustable parameters.

The layout of the paper is as follows. In the next section we present in outline the fundamentals of the EAM, the prescription for the determination of the pair potentials, and the parametrization procedure used in this work. We also present in outline the VMHNC theory and the thermodynamic relations needed in this work. In Sec. III we present the results for the liquid structure. Then we present the results for the thermodynamic properties (Helmholtz free energy, internal energy, and entropy) of the $3d$, $4d$, and $5d$ liquid transition metals near melting. We complete the paper, in Sec. IV, with a brief discussion of our results.

II. THEORY

A. Effective pair potential approximation from the embedded-atom method

In the EAM the energy of the metal is viewed as the energy to embed an atom into the local electron density provided by the remaining atoms of the system. In addition, there is a short-range core-core repulsion term. Whence the total energy of the system is written as

$$E=\sum_i F_i[\rho_H(r_i)]+\frac{1}{2}\sum_{i\neq j}\phi(r_{ij}). \tag{1}$$

In this expression F_i is the embedding energy for placing an atom into the host electron density ρ_H at the position r_i; ϕ is a short-range doubly screened repulsive pair interaction between quasiatoms i and j separated by a distance $r_{ij}=|\mathbf{r}_i-\mathbf{r}_j|$.

The host electron density is approximated by the linear superposition of atomic electron densities,[27]

$$\rho_H(r_i)=\sum_{j\neq i}\rho_j^a(r_{ij}), \tag{2}$$

where ρ_j^a is the atomic density of atom j at distance r_{ij} from the nucleus.

We follow Foiles[21] procedure for obtaining effective pair interactions from the EAM. This is briefly described below.

The embedding function $F(\rho)$ is replaced with a Taylor-series expansion about the average host density $\bar{\rho}$, where the electron density at site i is written as

$$\rho_{H,i}=\bar{\rho}+\sum_{j\neq i}[\rho_j^a(r_{ij})-\delta], \tag{3}$$

$\delta=\bar{\rho}/N-1$, and N is the number of atoms in the system. Expanding to second order, the EAM energy is approximated by

$$E=NE(\bar{\rho})+\frac{1}{2}\sum_{i\neq j}v(r_{ij}), \tag{4}$$

where

$$E(\bar{\rho})=F(\bar{\rho})-\bar{\rho}F'(\bar{\rho}), \tag{5}$$

and

$$v(r)=\phi(r)+2F'(\bar{\rho})\rho^a(r)+F''(\bar{\rho})[\rho^a(r)]^2 \tag{6}$$

defines the effective pair interaction used in this work. In the above equations $F'(\bar{\rho})$ and $F''(\bar{\rho})$ denote the first two derivatives of the embedding energy evaluated at $\bar{\rho}$.

We follow Foiles[21] in approximating $\bar{\rho}$ by the average electron density for a crystal with a lattice constant that matches the liquid density n. In the case of hcp crystals, we use the relation $c/a=k$ to obtain the atomic volume in terms of either a or c, with k taken from experiment.

In the EAM there are three functions to be specified, namely, the embedding energy as a function of the local electron density, the atomic electron density of each atom, and the screened electrostatic repulsion between the quasiatoms. It has been shown that, within the quasiatom approach, the rare-gas atoms have their lowest energies in a background of vanishing charge density and that the energies are linear in the density, while the chemically active elements have a linear region at high densities and a single minimum at lower densities.[28] Whence, we follow Daw and Baskes[1] in assuming that the embedding function $F(\rho)$ is zero for zero density and decreases to a single minimum at a value of ρ, which is slightly larger than the average electron density of the solid in equilibrium. The embedding functions are then determined by choosing functional forms meeting these general requirements and by adjusting them by fitting to some thermodynamic properties in the solid as discussed in Sec. III.

Turning now to our choice of the functional form of $\rho(r)$, we have found that electron densities obtained from Hartree-Fock calculations are unsatisfactory for the bcc transition metals. Adams and Foiles[22] reported similar difficulties and found the approach of Voter and Chen,[29] which we adopt in this work in its original form, more convenient for the study

TABLE I. Input thermodynamic data: ionic number density n and temperature T. EAM parameters A, α, and b and cutoff distances $r_{\rm cut}$ used in the determination of the effective pair interaction of liquid transition metals.

Metal	n (Å^{-3})	T (K)	A (10^3 eV)	α (Å^{-1})	b (Å^{-1})	$r_{\rm cut}$ (Å)
Sc	0.0391	1833	0.2	1.96	2.5	5.522
Ti	0.0522	1973	0.4	2.50	2.5	4.916
V	0.0634	2173	0.4	2.49	3.0	4.650
Cr	0.0726	2173	100	5.22	2.5	4.424
Mn	0.0654	1533	0.3	2.35	2.5	4.737
Fe	0.0756	1833	0.2	2.20	3.0	4.410
Co	0.0787	1823	3	3.90	2.5	4.213
Ni	0.0792	1773	3	3.80	2.5	4.645
Cu	0.0755	1423	3	3.80	2.5	4.763
Y	0.0287	1825	0.5	2.12	2.5	6.061
Zr	0.0392	2173	1.0	2.65	2.5	5.391
Nb	0.0493	2741	15.0	4.05	2.5	5.070
Mo	0.0586	2890	15.0	3.89	2.5	4.839
Tc	0.0540	2445	15.0	3.96	2.5	4.584
Ru	0.0649	2583	20.0	4.07	2.5	4.509
Rh	0.0594	1853	15.0	3.95	2.5	5.014
Pd	0.0594	1853	8.5	3.95	2.5	5.133
Ag	0.0518	1273	5.0	3.80	2.5	5.397
La	0.0258	1243	0.05	1.32	2.5	6.291
Hf	0.0405	2500	2.0	2.83	2.5	5.312
Ta	0.0499	3269	15.0	3.87	2.5	5.070
W	0.0580	3683	9.0	3.55	2.5	4.855
Re	0.0611	3453	10.0	3.65	2.5	4.628
Os	0.0636	3318	15.0	3.83	2.5	4.556
Ir	0.0607	2683	50.0	4.33	2.5	5.067
Pt	0.0577	2053	20.0	4.27	2.5	5.172
Au	0.0526	1423	5.0	3.70	2.5	5.384

of bcc transition metals. In this approach the contribution of each quasiatom to the total electron density is written as

$$\rho(r)=r^6[\exp(-br)+512\,\exp(-2br)], \tag{7}$$

where b is an adjustable parameter.

For the doubly screened electrostatic pair interaction $\phi(r)$ we choose the Born-Meyer function

$$\phi(r)=A\,\exp(-\alpha r), \tag{8}$$

where A and α are adjustable parameters. Several fitting procedures have been proposed in the literature for solid-state calculations, some more appropriate than others for a given crystalline structure. In this work, for the purposes of liquid-state calculations, the same procedure is applied to the three series of transition metals, irrespective of their parent crystallographic structure, which, given the isotropy of the liquid state, is a reasonable assumption. We lay no claim, however, to the appropriateness of the potentials for the calculation of solid-state properties. In fact, the embedding function has the wrong curvature for the calculation of the solid-state properties in three cases, as we indicate in Sec. III.

B. The VMHNC theory of liquids

The variational modified hypernetted chain (VMHNC) theory of liquids[3,4] pertains to a new generation of fairly accurate integral-equation theories of liquids. The suitability of the VMHNC for the specific case of liquid metals has been discussed elsewhere.[30,31] Like most liquid-state theories the VMHNC solves the Ornstein-Zernike (OZ) equation,[32] which relates the direct correlation function $c(r)$ to the pair distribution $g(r)$, within an approximate closure. The approximation is carried out at the level of the bridge function $B(r)$. Specifically, we use the analytic solution of the Percus-Yevick (PY) equation for hard spheres,[32] $B(r)=B_{\rm PY}^{\rm HS}(r;\eta)$, where the packing fraction $\eta=\eta(n;T)$ is the variational parameter, determined for each thermodynamic state by minimizing the VMHNC configurational Helmholtz free energy, $f^{\rm VMHNC}(T,n;\eta)$.[3,4] The value of $\eta=\eta(n;T)$ thus obtained is used to evaluate the bridge function which, in turn, is used to solve the OZ equation to calculate $g(r)$, the structure factor $S(q)$ and the thermodynamic properties. The Helmholtz free energy per atom, F, can be written as

$$F=F^{\rm ideal}+E(n)+k_BTf^{\rm VMHNC}, \tag{9}$$

where F^{ideal} is the ideal gas contribution and $E(n)$ is given by Eq. (5). The internal energy per atom U is given by

$$U=\frac{3}{2}k_BT+E(n)+2\pi n\int_0^\infty dr\ g(r)v(r), \qquad (10)$$

and the entropy S is written in terms of F and U through the thermodynamic relation $F=U-TS$.

III. RESULTS

A. Fitting procedure

We fitted the EAM functions to basic solid-state bulk properties, namely, the Voigt average bulk $\langle B\rangle_V$ and shear $\langle G\rangle_V$ moduli and the sublimation energy E_S as functions of the lattice parameter a (and of the c/a ratio in the case of the hcp metals). A similar fitting procedure was used by Oh and Johnson[33] in their EAM calculations for the fcc and hcp transition metals.

Cubic splines[34] were used to fit the embedding energies $F(\rho)$ with the curvatures set to zero at the end points. The parameters b of $\rho(r)$, A and α of $\phi(r)$, and the spline knots of $F(\rho)$ were determined by searching for parameters, which minimized the difference between calculated and experimental values.[35] Since the calculation of $\langle B\rangle_V$, $\langle G\rangle_V$, and E_S require the knowledge of all the three functions $\rho(r)$, $F(\rho)$, and $\phi(r)$ a number of sets of parameters A, α, and b and spline knots were found to give comparable fits to the experimental values. Following Adams and Foiles,[22] we chose the set of parameters that gave the best value for the Helmholtz free energy. We call this choice the optimum set of parameters. These values of A, α, and b are given in Table I. A table of values of the spline knots is available on request.

There appear to be no clear trends in the optimum set of parameters. Whereas the parameter b has the same value 2.5 Å^{-1} for all the transition metals, except for Fe, the parameters of the Born-Meyer potential exhibit large variations. We note, however, that the embedding function can only be determined up to a linear function of ρ. Hence, different looking sets of EAM functions may yield a similar energetics, and, rather than comparing the different embedding functions and pair interactions obtained by different choices of the parameters, it is preferable to compare the resulting effective interactions.[36]

The embedding energies for the three representative cases of V, Co, and Ni, which have bcc, hcp, and fcc structures, respectively, are shown in Fig. 1. There is, however, a serious difficulty in the cases of the three cubic metals for which the elastic constants $C_{12}<C_{44}$, namely Cr, Rh, and Ir, which we have not been able to overcome. Our fitting procedure yields $F''<0$ at the equilibrium electron density, which is contrary to the results of first-principles calculations.[28] We disregard this potential problem and plump for consistency by using the same fitting procedure for the whole set of liquid transition metals.

We assume that the effective interactions are significant only for the first three nearest-neighbor shells and cut off both $\rho(r)$ and $\phi(r)$ at the value r_{cut}, half way between the third- and fourth-nearest neighbors for all the transition metals (see Table I). We have adopted the same cutoff procedure as in Ref. 22, as it ensures the gradual cutoff of these functions. However, the choice of cutoff procedure affects the behavior of these functions, particularly at the nearest-neighbor sites, where the first two derivatives are important. Figure 2 shows that the same function $\rho(r)$, with the same value of the adjustable parameter b, results in somewhat different shapes of the function for different values of r_{cut}. Hence, the specific choice we have adopted plays a significant role in the results presented below. The effective pair potentials obtained by using the above cutoff procedure for liquids V, Co, and Ni are shown in Fig. 3. Once the above parametrization has been carried out, the ensuing body of theory for the calculation of liquid-state properties is parameter free.

B. Liquid structure

We present below the results for the calculations of the liquid structure $S(q)$ of the transition metals. These were

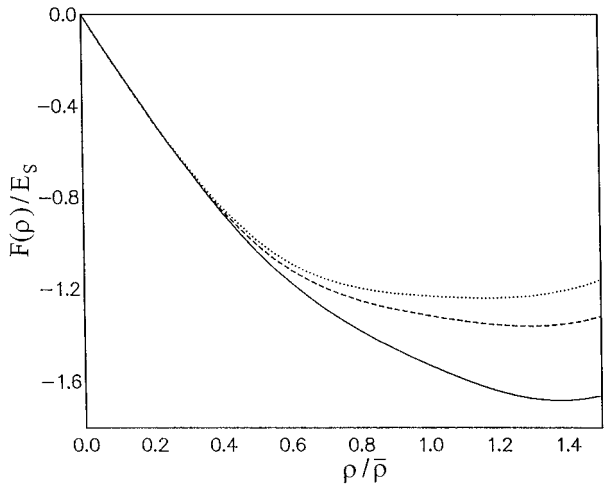

FIG. 1. Embedding energy functions $F(\rho)$ as a function of the electron density ρ. The energies are scaled by the sublimation energy and the density by the equilibrium density. Full line: V; dotted line: Co; broken line: Ni.

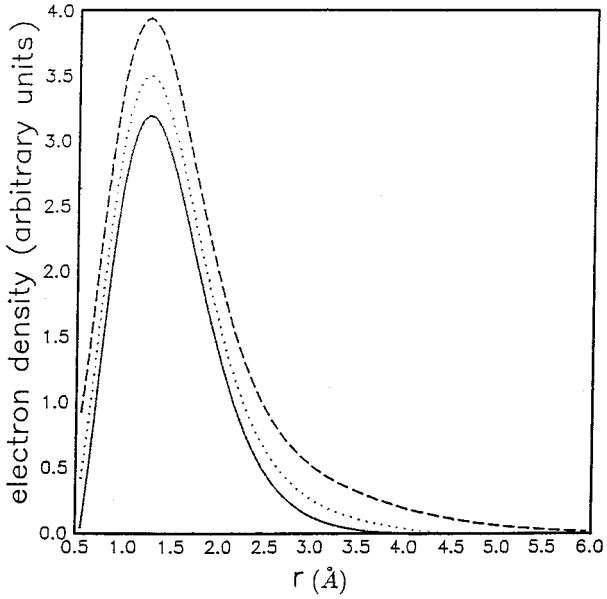

FIG. 2. Effect of the cutoff distance r_{cut} on the quasielectron density $\rho(r)$. In all cases $b=2.5$ Å. Broken line: no cutoff; full line: $r_{\text{cut}}=4.0$ Å; dotted line: $r_{\text{cut}}=4.74$ Å.

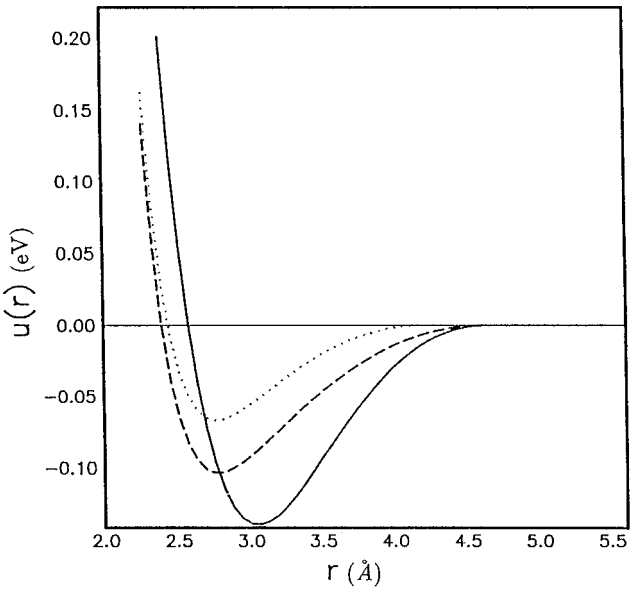

FIG. 3. EAM effective pair potentials. Full line: V; dotted line: Co; broken line: Ni.

carried out, within the VMHNC, using Gillan's algorithm.[37] In all cases we used a 1024-point grid with step size $\Delta r = 0.06$ Å. The input thermodynamic data used in our calculations are included in Table I.

Since the optimum set of parameters were chosen to give the best possible values for the Helmholtz free energy, there is no reason that these will result in a similarly good fit to the structure factor. It was therefore reassuring to find, as shown in Fig. 4 for Pd, that the choice of different sets of A, α, and b and spline knots has little effect on the liquid structure; the positions of the successive maxima remain almost unchanged, but there are small variations in their heights for different sets.

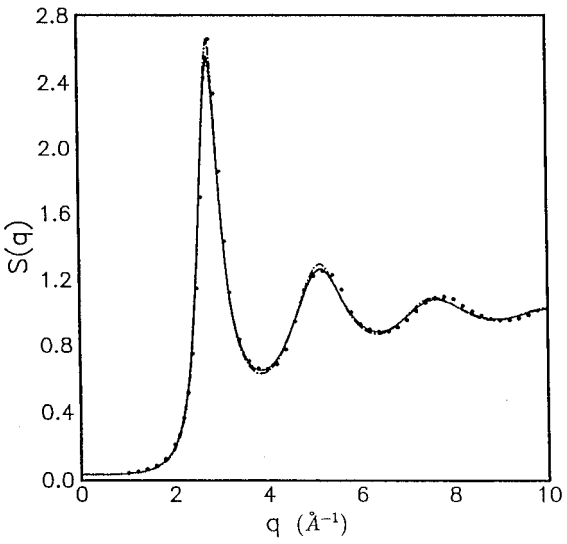

FIG. 4. Effect of the EAM parametrization on the liquid structure $S(q)$ of Pd. In all cases the cutoff distance is $r_{\rm cut}=5.1333$ Å. Full line: $A=8500$ eV; $\alpha=4.0$ Å^{-1}; $b=2.45$ Å^{-1}. Dash-dotted line: $A=10\,000$ eV; $\alpha=4.0$ Å^{-1}; $b=2.45$ Å^{-1}. Dotted line: $A=5000$ eV; $\alpha=3.8$ Å^{-1}. (The corresponding embedding energy functions are available on request.) Black circles represent the experimental data (Ref. 15).

Our choice of the optimum set of parameters and the cutoff procedure for both $\rho(r)$ and $\phi(r)$ have implications for the results of $S(q)$. Waseda and Tamaki[45] noted that the experimental data for the $3d$ series suggested a hardening of the repulsive effective potential cores, which they attributed to the filling of the $3d$ band. This, in turn, should be reflected as a trend in the parameters A and α, which is not present in our case and will affect the behavior of the oscillations beyond the principal peak of $S(q)$. The asymptotic behavior of the potential is reflected in the small q behavior of the liquid structure. The cutoff procedure implies an effective interaction of finite range [strictly $v(r)=0$ for a distance $R>r$], which probably underestimates the actual range of the interaction in transition metals and effectively determines $S(q)$ at small values of momentum transfer.

Figure 5 presents the results of the calculated $S(q)$ for those liquid transition metals for which experimental data are available.[15] Figure 5(a) shows the results for the $3d$ series, while Fig. 5(b) shows the results for the $4d$ and $5d$ series. In general, we find there is overall good qualitative agreement between calculated and experimental results. At a more detailed level, however, the following comments are in order.

The calculated $S(q)$ for the early $3d$ transition metals, Sc, Ti, and V, are rather poor when compared with experiment. The calculated $S(q)$ for Sc exhibits a shift towards smaller q's, while for the other two the shift is towards the larger q's. The heights of the successive peaks are only in moderate agreement with experiment, with Ti the worst case. Yet, with the exception of the results in Ref. 18, which uses three liquid structure adjustable parameters, our results are of comparable lack of quality as other calculations or simulations reported in the literature. Waseda noted that, of his set of experimental x-ray data of $S(q)$ for the $3d$ liquid transition metals, those for Ti and V are the least accurate.[15] We suggest there is a case for carrying out another set of experiments for liquids Ti and V.

With the exceptions of Pd, Ag, and Pt, where the calculated structure is in very good agreement with experiment, the calculations tend to overestimate the height of the principal peak of $S(q)$. Since the height and position of this peak is the result of a delicate balance between the repulsive and attractive contributions to the effective pair potential, this difference may be because of either the approximate theory of liquids VMHNC used in this work or the potential or to the combined effects of both. MD simulations using different EAM parametrizations show that these effective potentials tend to overestimate the height of the principal peak of $S(q)$,[21,25] whereas there is excellent agreement between the MD simulations and our VMHNC results. This suggests that the differences are mainly because of the effective potentials.

The overall qualititative agreement between the calculated and observed $S(q)$ discussed above, suggest that the liquid structures we calculated for those cases for which there is no experimental data may be be used with some degree of confidence. These $S(q)$, in tabular or graphic form, are available on request.

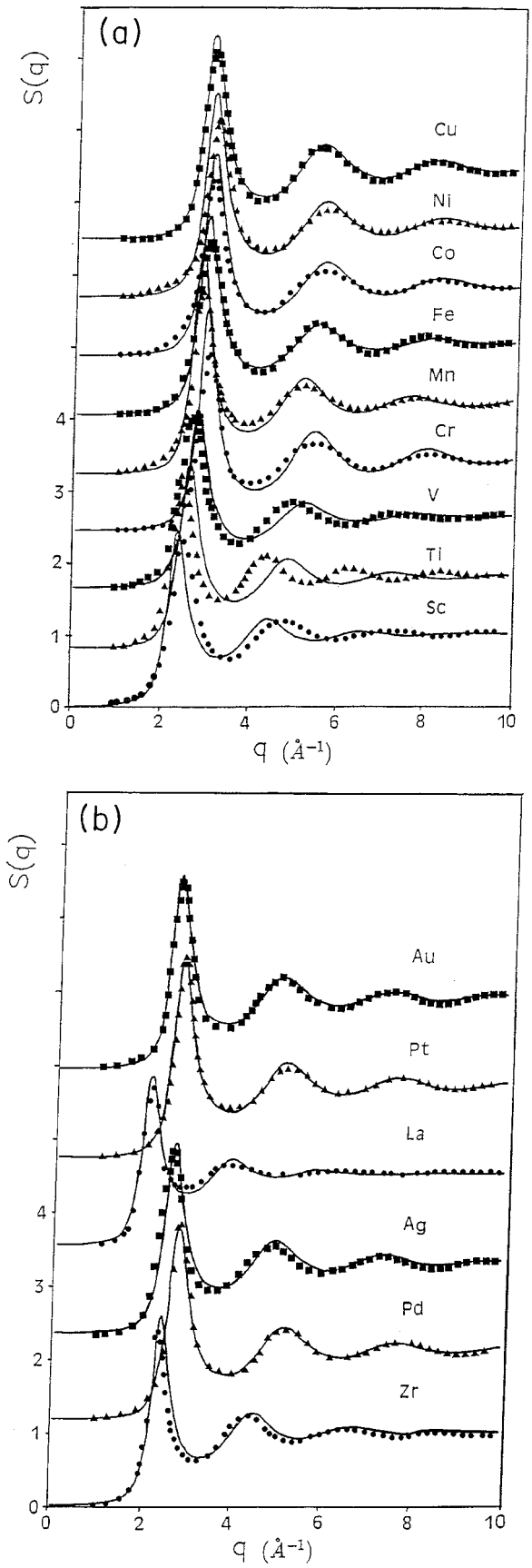

FIG. 5. Static structure factors of the liquid transition metals near melting (Table I). Solid lines: this work; full circles, triangles, and squares: experimental data (Ref. 15). (a) $3d$ row; (b) $4d$ and $5d$ rows. From bottom to top: Zr, Pd, Ag, La, Pt, and Au.

C. Thermodynamic properties

We now turn to the thermodynamic properties. A good theory of the liquid transition metals must be able to reproduce the well-established trends present in these properties. This is particularly so because the thermodynamic properties include, in addition to the effective pair potential, the important volume term contribution, $E(\overline{\rho})$, to E.

The results of our calculations of the Helmholtz free energy per atom, in eV, are presented in Fig. 6; 6(a) for the $3d$, 6(b) for the $4d$, and 6(c) for the $5d$, respectively. These are compared to the corresponding experimental data.[38] The excellent agreement between the two is not unexpected, given our choice of the optimum set of parameters. We must emphasize, however, that we have not fitted the parameters to the Helmholtz free energy. As stated in Sec. III A, out of the possible set of parameters and spline knots we have chosen the set that best reproduces the Helmholtz free energy. This choice of the optimum set of parameters, however, does not guarantee that the values obtained for the free energy will necessarily produce such an excellent agreement as shown in Fig. 6. Moreover, it appears that this is the main reason our calculations work in the liquid state. The results shown in this figure are made up of contributions of the volume term, which include $E(n)$ and the ideal gas contribution, and the structure-dependent terms. We note, see Table II, that the largest contribution to F comes from $E(n)$, which ranges from about 51% in Pd to 86% in Ti. The structure-dependent terms include contributions from both $S(q)$ [or $g(r)$] and the potential $v(r)$. Hence, there are large cancellations between F^{ideal} and the structure-dependent contributions to F. There is also subtle cancellation of errors arising from the use of finite range potentials and imperfections in the $S(q)$ obtained in our calculations and discussed in Sec. III B. Unlike $S(q)$, the results for F are sensitive to the choice of parameters that, in the specific case of Cr (taking $A=1000$ eV; $\alpha=3.0$ Å^{-1}; $b=2.8$ Å^{-1}), changes the value of F by about 15%.

Figure 7 shows the free energy per atom of liquid V as a function of temperature. The agreement between theory and experiment[38] is very good except near the boiling point, where the system has probably already undergone the metal-nonmetal transition. These results cover a range of over 700 K and are predictions of our theory using only the thermodynamic state as input data. We also note that our results are in agreement with the Monte Carlo simulations of LeSar, Najafabadi, and Srolovitz.[26]

We have also calculated the internal energy U for V from the temperature derivative of F and also, independently, by using Eq. (10). We find, for instance, that U at 2300 K is -4.57 eV, whereas the value obtained by using Eq. (10) at the same temperature is -4.50 eV. This reflects the internal consistency of our calculations.

The results of our calculations for the internal energy per atom U and the entropy per atom S are shown in Fig. 8: 8(a) for the $3d$, 8(b) for the $4d$, and 8(c) for the $5d$ rows near the melting points. U is evaluated by using Eq. (10) with the optimum set of EAM parameters and the thermodynamic state (T,n) as input data. Since there is no closed expression for S, this property is evaluated via the thermodynamic relation given at the end of Sec. II B.

The calculated values of U follow the experimental trends reasonably well,[38,39] but there are pronounced differences be-

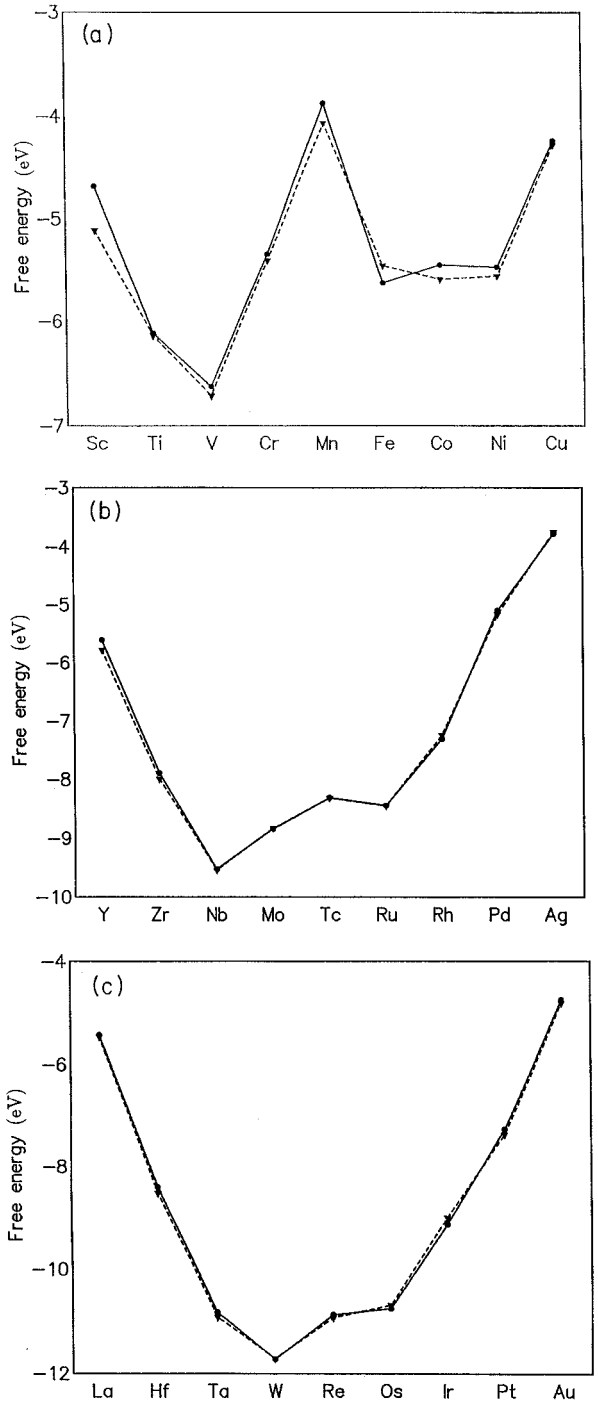

FIG. 6. Helmholtz free energies per atom of the three rows of liquid transition metals. Dots: this work; triangles: experimental values (Ref. 38). The solid line joining the dots and broken lines joining the triangles are a guide to the eye. (a) 3*d* series; (b) 4*d* series; (c) 5*d* series.

tween theory and experiment, particularly around the middle of the rows, where the effects of electron correlation on cohesion are believed to be important.[40] As in the case of F the main contribution comes from $E(n)$. The contributions due to the correlations between the atoms [last term in Eq. (10)] is typically around -0.5 eV or less, whereas the kinetic energy contribution ranges from about 0.16 eV for La to 0.48 eV for W. Although one of the fitting parameters is the sublimation energy E_S, the difference between U and E_S is, in all cases, larger than the kinetic energy. Given the cancellation, which takes place between the kinetic energy and correlation contributions, there is no *a priori* reason to expect the reasonable agreement between theory and experiment shown in Fig. 8. The atom-atom correlation contribution is probably the most important term in deciding whether there is a good agreement between theory and experiment. However, great care has to be exercised in the interpretation of results. The agreement between calculated and experimental values of U for V and Pd is quite good. Yet only for Pd do we find a very good agreement between calculated and experimental $S(q)$. This points to subtle cancellation of errors between the contribution of the potential and the structure. To clarify this point, we have compared our results for the internal energy with those obtained for some metals from MD simulations; this is shown in Fig. 9. The simulations use different EAM parametrizations and also include the multiple-atom contributions to the interatomic potentials. Yet, our VMHNC results are in good agreement with, and are bracketed by, the simulation results. Both exhibit similar dis-

TABLE II. The structure-independent part of the total energy $E(n)$ and the Helmholtz free energy F for liquid transition metals (three taken from each series, which have hcp, bcc, and fcc structures in the solid phase).

Series	System	F/eV	$E(n)$/eV
3*d*	Ti	−6.116	−5.247
	Cr	−5.341	−3.212
	Ni	−5.470	−3.806
4*d*	Zr	−7.893	−6.332
	Mo	−8.863	−7.344
	Pd	−5.104	−2.590
5*d*	Hf	−8.403	−6.626
	W	−11.726	−9.388
	Pt	−7.278	−4.169

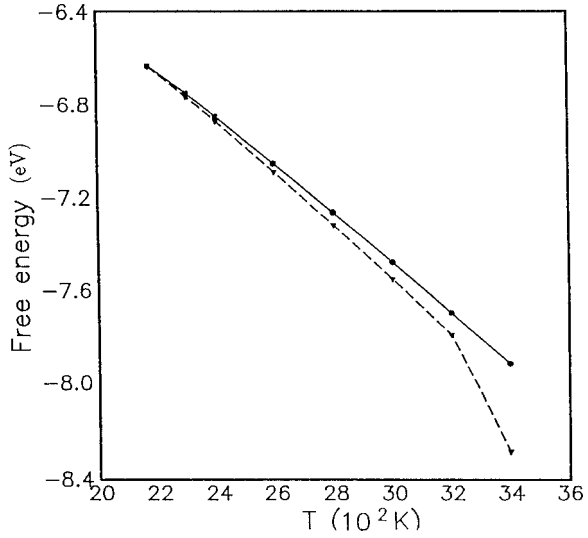

FIG. 7. Temperature dependence of the Helmholtz free energy of liquid vanadium. Dots joined by full lines: this work; triangles joined by broken lines: experiment (Ref. 38).

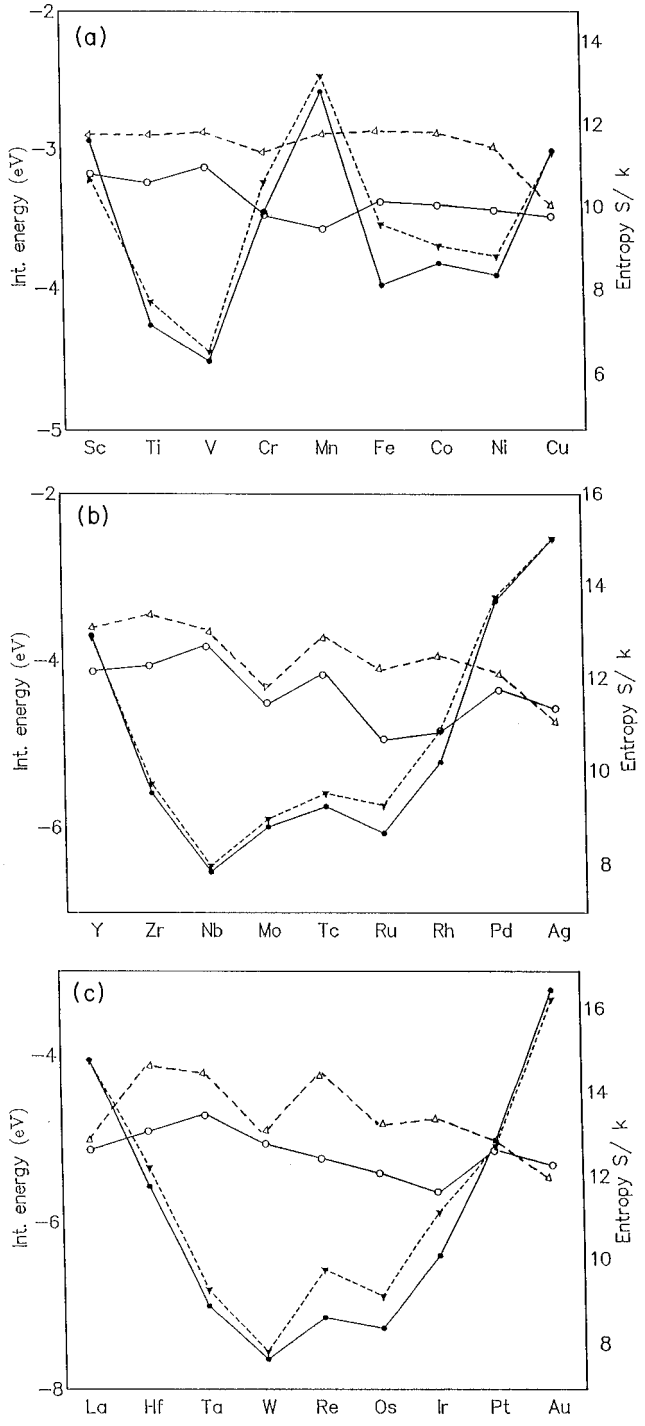

FIG. 8. Internal energies and entropies per atom of the three rows of liquid transition metals. Dots: this work (full dots: internal energy; empty dots: entropy); triangles: experimental data [full triangles: internal energy (Refs. 38 and 39); empty triangles: entropy (Ref. 39)]. The solid lines joining the dots and broken lines joining the triangles are a guide to the eye. (a) $3d$ series; (b) $4d$ series; (c) $5d$ series.

crepancies with experiment. We conclude that the differences between theory and experiment are likely to be because of the EAM effective potential.

Turning now to the results for the entropy per atom, in units of k_B, we note that while the calculated values follow roughly the trends of the experimental values[39] across the

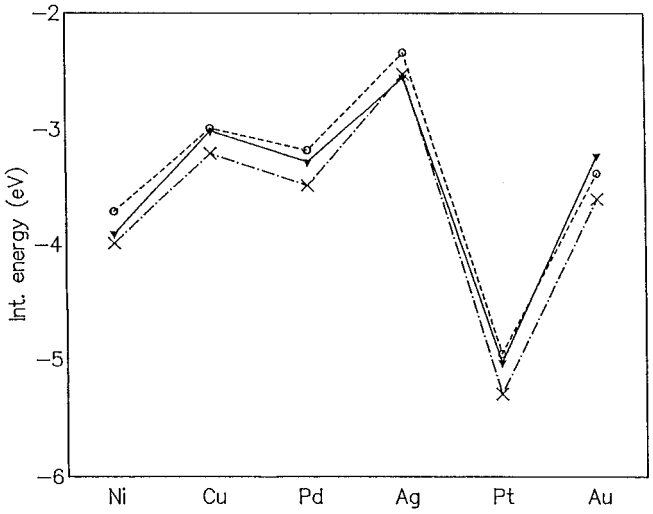

FIG. 9. Comparison between the internal energies calculated in this work and those obtained from ML simulations for a few transition elements. In all cases the EAM has been used. Triangles and full lines: this work; circles and broken lines: Ref. 21; crosses and dash-dotted lines: Ref. 25.

series, the former are generally too small, in some case by as much as $2k_B$. Normally results are presented in terms of the excess entropy, $S^E = S - S^{\text{ideal}}$, but in our case using S has helped us to analyze the trends discussed below, and we decided to present our results in this way. This has allowed us to compare our results to those in Refs. 41 and 42 directly (see below). The calculated S^E is normally flatter compared to the experimental results. For the $3d$ series, the $-S^E$ calculated values vary from 2.8 for V to 3.9 for Mn, whereas the experimental values vary from 1.6 for Mn to 3.4 for Cu. We also note that for Pd there is also a difference between the calculated and experimental S even though we find excellent agreement for both F and U. However, the differences between the calculated and experimental values do not depend strongly on temperature, as illustrated in Fig. 10 for vanadium. Hence, our results will predict reasonably good values

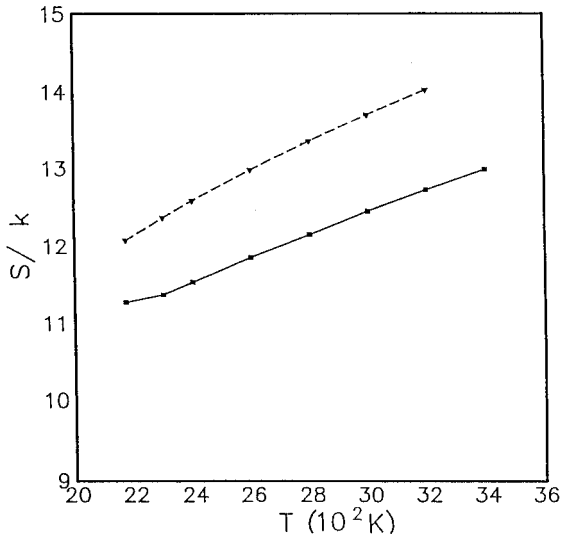

FIG. 10. Same caption as Fig. 7 but for the entropy per atom. The experimental data shown are taken from Ref. 39.

TABLE III. EAM results for entropies per atom in units of k_B and their differences from experimental values for $3d$ liquid transition metals [MSY stands for Meyer, Stott, and Young (Ref. 41) and IS for Itami and Shimoji (Ref. 42)].

System	S/k_B (cal)	S/k_B (expt)	$(S_{\text{expt}}-S_{\text{cal}})/k_B$	S_{elec}/k_B (MSY)	S_{elec}/k_B (IS)
Sc	11.092	12.050	0.958		0.920
Ti	10.889	12.010	1.121	1.685	0.810
V	11.273	12.080	0.962	1.539	0.830
Cr	10.098	11.580	1.538	1.585	0.800
Mn	9.773	12.050	2.280	2.555	0.670
Fe	10.417	12.110	1.766	2.062	0.900
Co	10.346	12.080	1.808	2.203	0.970
Ni	10.210	11.690	1.580	1.699	1.090
Cu	10.042	10.270	0.276		0.095

for the heat capacity at constant pressure C_P. In fact we have estimated that for V, at $T=2350$ K, $C_P \cong 7.6$ cal K^{-1} mol^{-1}, whereas the experimental value is 9.7 cal K^{-1} mol^{-1}. We argue below that, at least in part, the differences between the calculated and experimental values of the entropy are because we ignore the electronic contribution to the entropy. Our argument has to be moderated by the fact that, in some cases, such as Ni in the $3d$ series considered below, the magnitude of the difference between calculated and experimental entropies is larger than S^E.

Mayer, Stott, and Young[41] (MSY) and Itami and Shimoji[42] (IS) have shown that the electronic contribution to the entropy, S_{el}, of liquid transition metals is not negligible. S_{el} is proportional to the density of the extended electron states at the Fermi level, and both MSY and IS made estimates of the contributions of S_{el} to the total entropy of the $3d$ row. These values are shown in Table III. We note that the deficits in our calculated entropies, which are also shown in Table III, are bracketed between the IS and MSY results. Recent calculations of the density of states of Mn, Fe, Co, and Ni,[18,43] which are in good agreement with those deduced from the experimental data,[44] give values of S_{el} nearer to IS. Moreover, revisiting the temperature dependence of the entropy deficit for V, illustrated in Fig. 10, we observe that $\Delta S \propto T$, which is in accord with the interpretation of ΔS as the electronic contribution to the entropy, ignored in our calculations. The results in Fig. 10 are consistent with the density of states at the Fermi level $\approx$20 electrons/atom Ry.

IV. DISCUSSION AND CONCLUSIONS

The results presented in the preceding section are in reasonably good qualitative agreement with the experimental structures, free and internal energies, and entropies of the three series of the liquid transition metals. The calculations were carried out using EAM-derived effective pair potentials with parameters fitted to solid-state data together with the VMHNC theory of liquids, in a formalism otherwise free of adjustable parameters. The EAM parametrization we have adopted in this work has some problems; these were discussed in Sec. III A. However, even if there were no problems, parametrizing to solid-state data does not guarantee good effective pair potentials for the liquid state. For instance, the careful parametrization procedure used in Ref. 22, predicts an amorphous rather than liquid structure for vanadium in the liquid state near melting. Ideally we would wish to produce a theory that gives effective potentials capable of predicting with reasonable accuracy both solid- and liquid-state properties. Unfortunately we have not reached this level of understanding of transition metals. Whereas solid-state properties are calculated with reference to the bottom of the potential well, liquid-state properties depend on a delicate balance between the kinetic and potential energy contributions, and a detailed knowledge of the effective potential is required. The choices of parametrization are dictated by this fundamental consideration.

Comparison between the results of the VMHNC theory and MD simulations for equivalent potentials show that the former is very accurate for the study of liquid transition metals. Since the simulations normally include multiatom contributions to the effective potential, our results suggest that the effective pair potential is a very good approximation for the study of liquid-state properties. This is in agreement with Moriarty's conclusions using GPT effective potentials.[12]

ACKNOWLEDGMENTS

It is a pleasure to thank Jean-Louis Bretonnet, David Gonzalez, Ana Serra, Çetin Tasseven, Hugh Young, and Yoshio Waseda for several useful discussions during the course of this work. We are also grateful to the third named for assistance with her expertise in handling systems with hcp solid structure. One of us (G.M.B.) gratefully acknowledges the Commonwealth Scholarship Commission for support.

*Author to whom all correspondence should be addressed.

[1] M. S. Daw and M. I. Baskes, Phys. Rev. Lett. **50**, 1285 (1983); Phys. Rev. B **29**, 6443 (1984).
[2] M. W. Finnis and J. E. Sinclair, Philos. Mag. A **50**, 45 (1984).
[3] Y. Rosenfeld, J. Stat. Phys. **42**, 437 (1986).
[4] L. E. Gonzalez, D. J. Gonzalez, and M. Silbert, Phys. Rev. A **45**, 3803 (1992).
[5] J. M. Wills and W. A. Harrison, Phys. Rev. **28**, 4363 (1983).

[6] C. Hausleitner and J. Hafner, J. Phys. F **18**, 1025 (1988).
[7] J. L. Bretonnet and A. Derouiche, Phys. Rev. B **43**, 8924 (1991).
[8] C. Regnaut, Z. Phys. B **76**, 179 (1989).
[9] C. Hausleitner, G. Kahl, and J. Hafner, J. Phys: Condens. Matter **3**, 1589 (1991).
[10] J. A. Moriarty, Phys. Rev. B **38**, 3199 (1988); **42**, 1609 (1990).
[11] One of us (G.M.B.) attempted to evaluate the liquid structure using the pairwise contribution to the Moriarty potential (Ref. 10) and incorporating the three-body contribution in an approximate manner. The calculations for the liquid structure, using as input the experimental melting-point density and temperature, failed to converge to a result even for liquid Ni.
[12] J. A. Moriarty, Phys. Rev. B **49**, 12 431 (1994).
[13] J. L. Bretonnet and M. Silbert, Phys. Chem. Liq. **24**, 169 (1992).
[14] G. M. Bhuiyan, J. L. Bretonnet, L. E. Gonzalez, and M. Silbert, J. Phys: Condens. Matter **4**, 7651 (1992); G. M. Bhuiyan, J. L. Bretonnet, and M. Silbert, J. Non-Cryst. Solids **156–158**, 145 (1993).
[15] Y. Waseda, *The Structure of Non-Crystalline Materials* (McGraw-Hill, New York, 1981).
[16] Ç. Tasseven, G. M. Bhuiyan, and M. Silbert (unpublished).
[17] For an interesting discussion, see, cf., N. H. March, AERE Harwell Report No. TP981 (1983).
[18] L. Do Phuong, A. Pasturel, and D. Nguyen Manh, J. Phys: Condens. Matter **5**, 1901 (1993).
[19] M. J. Stott and E. Zaremba, Solid State Commun. **32**, 1297 (1979); Phys. Rev. B **22**, 1564 (1980); J. K. Norskov and N. D. Lang, *ibid*. **21**, 2131 (1980).
[20] F. Aryasetiawan, M. Silbert, and M. J. Stott, J. Phys. F **16**, 1419 (1986).
[21] S. M. Foiles, Phys. Rev. B **32**, 3409 (1985).
[22] J. B. Adams and S. M. Foiles, Phys. Rev. B **41**, 3316 (1990).
[23] J. M. Holender, Phys. Rev. B **41**, 8054 (1990); J. Phys: Condens. Matter **2**, 1291 (1990).
[24] J. Mei and J. W. Davenport, Phys. Rev. B **42**, 9682 (1990).
[25] L. M. Holzman, J. B. Adams, S. M. Foiles, and W. N. G. Hitchen, J. Mater. Res. **6**, 298 (1991).
[26] R. LeSar, R. Najafabadi, and D. J. Srolovitz, J. Chem. Phys. **94**, 5090 (1991).
[27] It appears that the approximation of additive atomic densities was introduced in R. G. Gordon and Y. S. Kim, J. Chem. Phys. **56**, 3122 (1971).
[28] M. J. Puska, R. M. Nieminen, and M. Manninen, Phys Rev. B **24**, 3037 (1981).
[29] A. F. Voter and S. P Chen, in *Characterization of Defects in Materials*, edited by R. W. Siegel, J. R. Weertman, and R. Sinclair, MRS Symposia Proceedings No. 82 (Material Research Society, Pittsburgh, 1987), p. 175; S. P. Chen, D. J. Sroloviz, and A. F. Voter, J. Mater. Res. **4**, 62 (1989).
[30] L. E. Gonzalez, A. Meyer, M. P. Iñiguez, D. J. Gonzalez, and M. Silbert, Phys. Rev. E **47**, 4120 (1993).
[31] L. E. Gonzalez, D. J. Gonzalez, M. Silbert, and J. A. Alonso, J. Phys C: Condens. Matter **5**, 4283 (1993).
[32] See, c.f. N. H. March and M. P. Tosi, Atomic Dynamics in Liquids (Macmillan, London, 1976).
[33] D. J. Oh and R. A. Johnson, J. Mater. Res. **3**, 471 (1988).
[34] W. H. Press, S. A. Teukolsky, W. T. Vetterling, and B. P. Flannery, *Numerical Recipes in Fortran*, 2nd ed. (Cambridge University Press, Cambridge, England, 1992).
[35] The sources of the experimental data used are as follows. For the Voigt average bulk and shear moduli $\langle B\rangle_V$ and $\langle G\rangle_V$ and the sublimation energies E_S, we have used G. Simmons and H. Wang, *Single Crystal Elastic Constants and Calculated Aggregate Properties: A Handbook*, 2nd ed. (MIT Press, Cambridge, Massachusetts, 1971); K. A. Gschneider, Solid State Phys. **16**, 275 (1964). For the values of the lattice constants a and c we have used C. Kittel, *Introduction to Solid State Physics*, 5th ed. (Wiley, New York, 1976); W. B. Pearson, *Handbook of Lattice Spacing and Structures* (Pergamon New York, 1967), Vol. 2; R. W. G. Wyckoff, *Crystal Structures*, 2nd ed. (Wiley, New York, 1963), Vol. 1. For the liquid densities n we have used R. C. Weast, *Handbook of Chemistry and Physics*, 70th ed. (CRC, Boca Raton, 1989); G. R. Gathers, Rep. Prog. Phys. **49**, 341 (1986); Y. Waseda, *The Structure of Non-Crystalline Materials* (Ref. 15).
[36] M. S. Daw (unpublished).
[37] M. J. Gillan, Mol. Phys. **39**, 839 (1979).
[38] R. Hultgren, *Selected Values of Thermodynamic Properties of Elements* (American Society for Metals, Ohio, 1973).
[39] I. Barin, O. Knacke, and O. Kubaschewski, *Thermodynamic Properties of Inorganic Substances* (Springer-Verlag, Berlin, 1973), Suppl.
[40] C. M. Sayers, J. Phys. F **7**, 1157 (1977).
[41] A. Mayer, M. J. Stott, and W. H. Young, Philos. Mag. **33**, 381 (1976).
[42] T. Itami and M. Shimoji, J. Phys. F **14**, L15 (1984).
[43] W. Jank, Ch. Hausleitner, and J. Hafner, J. Phys C **3**, 4477 (1991).
[44] G. Buch and H. J. Guntherodt, *Solid State Physics*, edited by H. Ehrenreich, F. Seitz, and D. Turnbull (Academic, New York, 1974), Vol. 29, p. 235.
[45] Y. Waseda and S. Tamaki, J. Phys. F **6**, L89 (1976).